

The emission distribution in RR Pictoris

L. Schmidtbreick^{(1)*}, C. Tappert^{(2)†}, and I. Saviane^{(1)‡}

¹*European Southern Observatory, Casilla 19001, Santiago 19, Chile*

²*Grupo de Astronomía, Universidad de Concepción, Casilla 160-C, Concepción, Chile*

Accepted xxxx. Received xxxx; in original form xxxx

ABSTRACT

We present time-resolved optical spectroscopy of the old nova RR Pic. Two emission lines ($H\alpha$ and He I) are present in the observed part of the spectrum and both show strong variability. $H\alpha$ has been used for Doppler tomography in order to map the emission distribution in this system for the first time. The resulting map shows the emission from the disc as well as two additional emission sources on the leading and trailing side of the disc. Furthermore we find evidence for the presence of either a disc-overflow or an asymmetric outflow from the binary with velocities up to $\pm 1200 \text{ km s}^{-1}$. The origin of the outflow would be the emission source on the leading side of the accretion disc.

Key words: Physical data and processes: accretion, accretion discs – stars: novae, cataclysmic variables – individual: RR Pic.

1 INTRODUCTION

Cataclysmic Variables (CVs) are close, interacting binary systems, comprising a white dwarf receiving mass from a Roche-lobe-filling late-type star. In absence of strong magnetic fields, the mass transfer takes place via an accretion disc. RR Pic belongs to the subclass of CVs known as classical novae, which have displayed a thermonuclear runaway outburst. The system has been discovered by Spencer Jones (1931) at maximum light in 1925 and, although it was of slow type, it is supposed to be in its quiescence state by now. The orbital period of 0.145025 days (Vogt 1975) places it just above the period gap of CVs. Vogt found the lightcurve dominated by a very broad hump, often interrupted by superimposed minima. He explained this behaviour by an extended hot spot region with an inhomogeneous structure. Haefner & Metz (1982) however, explained their own time-resolved photometric and polarimetric observations together with radial velocity variations of the He II (4686 \AA) emission line (Wyckoff & Wehinger 1977) by suggesting the presence of an additional source of radiation opposite the hot spot. From high speed photometry, Warner (1986) concluded that during the 1970s (about 50 yr after outburst) structural changes have taken place in the system, resulting in a more isotropic distribution of the emitted radiation. In addition, he has found evidence for a shallow, irregular eclipse, showing RR Pic to be a high inclination system. Haefner & Betzenbichler (1991) confirmed the general

change in the lightcurve of RR Pic as well as the presence of the eclipse, which they found to be very stable over several orbits. However, they point out that the additional emission source on the trailing side is still necessary to understand the phase relation between the radial velocity curve and the photometric lightcurve.

Apart from this, the question arose whether RR Pic is an intermediate polar. Additional to the orbital period, Kubiak (1984) found a periodic modulation in the optical with a 15 min period. He interpreted this as the rotation of the white dwarf and concluded that RR Pic is an intermediate polar. Haefner & Schoembs (1985) however, repeated the high time-resolved photometry on a longer time-scale and could not find any sign of this short period. Since no 15 min period variation is found in X-ray measurements (Becker & Marshall 1981) either, they concluded that Kubiak's variation was more likely a transient event in the disc rather than a rotating white dwarf. Also Warner's high-speed photometry does not reveal any period other than the orbital one. Hence no evidence remains that RR Pic is an intermediate polar.

With a quiescence magnitude $m_V = 12$ mag, RR Pic is a comparatively bright CV. Although it has been well observed photometrically, spectroscopic studies of the binary are sparse. In particular, no systematic investigation of the line profile has been undertaken so far, which could provide information on the accretion process in this system. In this paper we present new time-resolved spectroscopic data on RR Pic and compare it with photometric data from the literature. We establish a Doppler map of the $H\alpha$ emission, study the isolated emission sources in the disc, and discuss the models of RR Pic's accretion disc. Finally, we analyse

* lschmidt@eso.org

† claus@gemini.cfm.udec.cl

‡ isaviane@eso.org

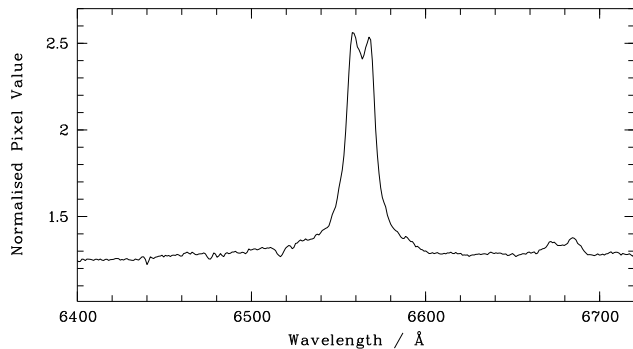


Figure 1. The 19 individual spectra have been added up and divided by the mean continuum to produce this average, normalised spectrum. Only the part around H α (6563 Å) and He I (6678 Å) is plotted.

the high velocity wings of the H α line and discuss possible interpretations.

2 DATA

The time-resolved optical spectroscopy was obtained on 2002 February 23 with the Boller & Chivens at the 1.52m ESO telescope on La Silla. Grating #20 together with a 1.5 arcsec slit has been used to cover the wavelength range from 5800 to 7500 Å with a spectral resolution of 2.45 Å FWHM. 19 spectra were obtained, each with an exposure time of 600 s. In total, we cover 3.8 h, which is slightly more than a complete orbit. IRAF has been used for the basic data reduction including BIAS subtraction, flat-fielding, and wavelength calibration. No flux calibration has been performed. Two emission lines (H α and He I) are present in the observed part of the spectrum. Both lines show a double peak profile in the average spectrum of all exposures (Fig. 1) and strong variability in time (Fig. 2). H α has been used for further analysis in order to map the emission distribution in the system, thus gaining insight in the accretion structure and additional components. For this we used the tomography code by Spruit (1998), with a MIDAS interface replacing the original IDL routines (Tappert et al. 2002).

Note, that this technique makes use of the variability of the line due to the binary rotation. We also expect a contribution to the line of the extended remnant shell of RR Pic which expands with a velocity around 400 km s⁻¹ (Rosino et al. 1982). However, since the shell is a circumbinary object, it is not effected by the binary rotation and any contribution to the line profile is a stable one. It does therefore not effect the here presented study.

3 DISCUSSION

3.1 Orbital period and zero phase

The radial velocities have been determined by applying the double Gaussian method as described in Shafter (1983). To evaluate the orbital period, two broad Gaussians have been fitted to each H α line. The Scargle algorithm (Scargle 1982)

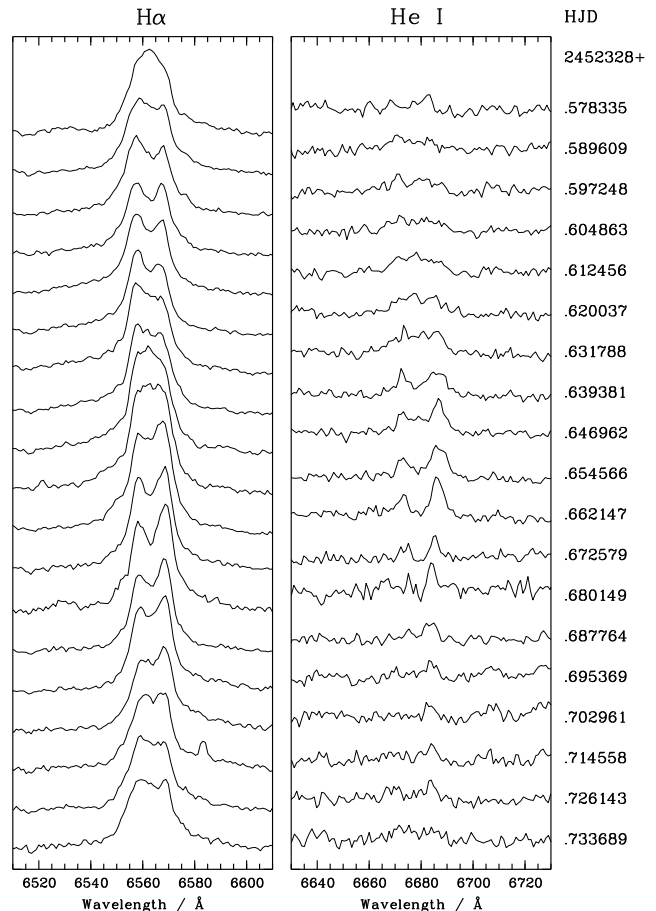


Figure 2. The time-resolved sequence of the two emission lines H α (6563 Å) and He I (6678 Å) is plotted. Note that the scaling of the two plots is different to ensure maximal visibility of both lines. The little feature on the red side of H α at epoch .714568 is an artefact due to a not properly subtracted cosmic ray.

as implemented in MIDAS has been used to find the period in the radial velocities. As expected for data that covers one orbit only, the periodogram shows a broad maximum at $P = 0.151$ d. This maximum also includes the value of $P = 0.1450255(2)$ d, which Vogt (1975) has found from time-resolved photometry. We hence use this much more precise value for the further analysis.

To compare the observed spectral features with the photometric lightcurves in the literature, it is essential to synchronise the respective phases. Unfortunately, Vogt's measurements are too far away in time from our observations for the accuracy of the period to yield an unambiguous zero phase. However, Kubiak (1984) later showed the constancy of the period and even improved the value slightly, in addition Warner (1986) and Haefner & Betzenbichler (1991) agree on the stability of the eclipse. Bringing these information together, we finally made use of Warner's lightcurve S3464 from December 1984 (Warner 1986), determined its HJD of the eclipse as zero point, and added Kubiak's period to create the ephemeris

$$\text{eclipse} = \text{HJD}2450064.441(2) + 0.14502545(7) \cdot E, \quad (1)$$

with E being the number of cycles. These values are of suf-

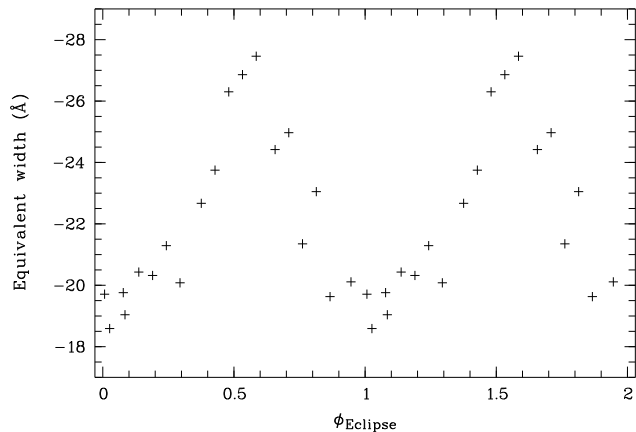


Figure 3. Equivalent width of H α plotted against photometric eclipse phase. Due to its breadth, the minimum at $\phi_E = 1$ is unlikely to represent an eclipse.

ficiently high accuracy to be extrapolated and compared to our observations. Defining the zero phase $\phi_E = 0$ as the time of the eclipse we derive the orbital phase ϕ_E for each observational point as

$$\phi_E = \frac{\text{HJD}_{\text{obs}} - 2450064.441}{0.14502545} + E \quad (2)$$

Our observation starts $E = 15612$ cycles after Warner’s S3464 lightcurve. For the zero phase we hence derive an uncertainty of $\sigma_0 = 0.003$ d or 0.02 phases. For comparison with Fig. 2, the first observation (HJD = 2452328.578335) was obtained at phase $\phi_E = 7 \cdot 10^{-5}$, the typical time between two exposures is equivalent to 0.053 phase units.

3.2 Equivalent width

In Fig. 3, the equivalent width of the H α -line has been plotted against the orbital phase as derived from Equation 2. A clear sinusoidal variation with a broad minimum around 1.0 and maximum around 0.5 orbits is detected. This behaviour agrees with measurements of the equivalent width by Haefner & Betzenbichler (1991).

A comparison with published lightcurves (Haefner & Metz (1982), Warner (1986), and Haefner & Betzenbichler (1991)) shows that the broad maximum in the lightcurves, which is partly eclipsed, does not coincide with maximal H α emission, but rather with the broad minimum of the equivalent width. This indicates that it is probably caused by a region with enhanced continuum radiation, which is hence more optically thick, and therefore suppresses the H α emission from this part of the disc. The maximal H α flux instead comes from a region situated on the opposite side of the disc and coincides with the start of the minimum at $\phi_E = 0.7$ (named No1 by Warner) of the lightcurve.

Important for the later computation of the Doppler maps is the fact that, within the errors of the equivalent width, no eclipse feature is found in the line. Hence, all data can be used for the Doppler tomography. Still, the variation of equivalent width requires a careful handling, which is discussed in more detail in the corresponding section.

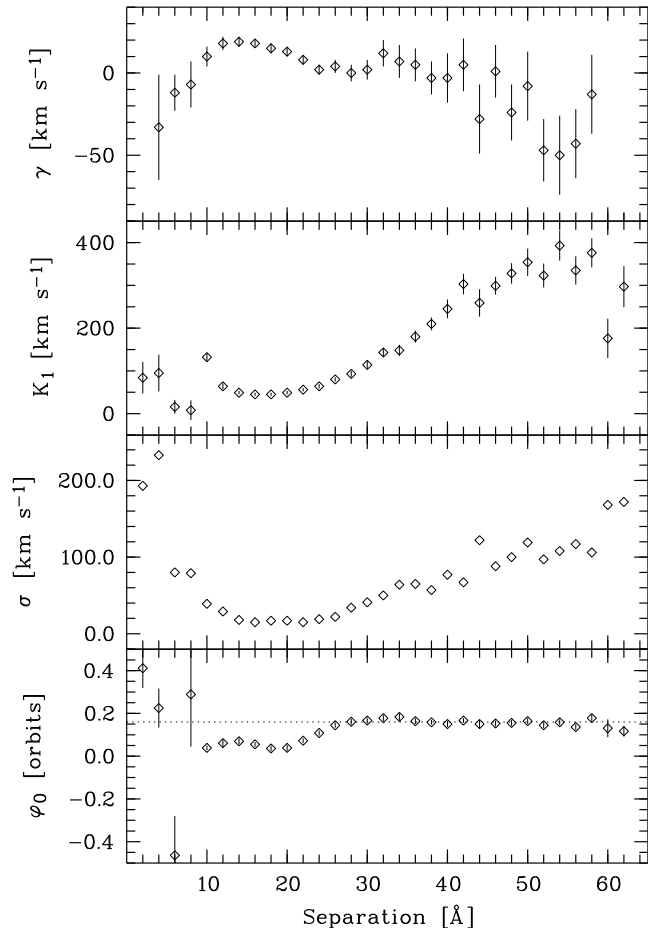


Figure 4. Diagnostic diagram for RR Pic showing the parameters of the radial velocity fit as function of the Gaussian separation. The phases of the radial velocities were calculated with respect to the eclipse ephemeris ϕ_E . The ϕ_0 plot therefore gives the difference between ϕ_E and the zero point of the radial velocity fit. The dotted line indicates the adopted correction resulting from the diagnostic diagram.

3.3 Diagnostic Diagram

While broad Gaussians have been sufficient to measure the orbital period, greater care must be taken to determine those radial velocities, which shall be used to study the line profile in more detail and to derive orbital parameters. As the motion of the white dwarf should be best represented by the extreme high-velocity line wings, which originate from the innermost part of the disc, one aims for a maximum separation of the two Gaussians without being contaminated by the continuum noise. This is usually achieved by a diagnostic diagram (Shafter 1983) as shown in Fig. 4, where the parameters of the radial velocity fit,

$$v_r(\phi) = \gamma - K_1 \sin 2\pi\phi, \quad (3)$$

are plotted as a function of the separation of the two Gaussians. The FWHM of each Gaussian was chosen to be 2\AA . The amplitude K_1 shows an extremely steep slope to higher velocities with separation d and reaches a maximum value of about 350 km s^{-1} . Although high values of K_1 might be expected from a high inclination system such as RR Pic, the

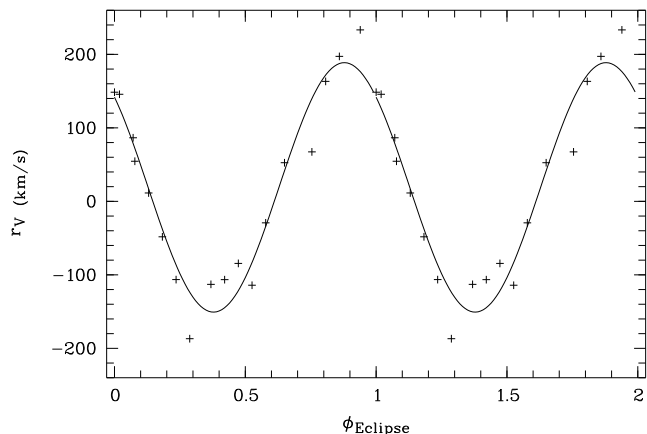


Figure 5. The radial velocities determined with the separation $d = 34$ of the double Gaussian are plotted against the orbital phase. The line indicates the best sinusoidal fit to the data. The semi-amplitude for this separation is $K_1 = 169.7 \pm 7 \text{ km s}^{-1}$. The offset in radial velocities can be explained by the system velocity γ , the offset between zero phase of radial velocity and photometric eclipse is discussed in the text.

value derived in this case is very improbable if not impossible. With $K_1 = 350 \text{ km s}^{-1}$ and $P = 0.145 \text{ d}$ the distance for the white dwarf to the centre of mass is 0.9 solar radii. The maximum possible distance between white dwarf and secondary for a CV with this period is roughly 1.6 solar radii. Hence, the centre of mass would be situated nearer to the secondary than to the primary, which would imply a mass ratio $M_2/M_1 > 1$, and does not allow for a stable mass transfer. Additionally, we point out that the maximum values of K_1 are reached at very high separations, which are already far away from the line centre in a region of very low S/N. We conclude that even at high separation, the line is still affected by additional emission sources, which then must be large and reach either deep into the central part of the disc or do not belong to the disc at all, as discussed in section 3.5.

As a consequence of the steep increase of K_1 , the ordinarily plotted ratio $\sigma(K_1)/K_1$ stays nearly constant and can not be used to indicate maximal possible separation. We instead plot the error of the sinusoidal radial velocity fit σ to give an idea of the uncertainties. The strong variation that starts around $d \sim 34$ might indicate the point of optimal separation and favours a semi-amplitude $K_1 \sim 170 \text{ km s}^{-1}$. In Fig. 5 the radial velocities for $d = 34$ are plotted against the orbital phase.

After the initial distortion due to the double peaked line profile (Tappert 1999) the zero phase settles at a value around 0.05 between separations $d \approx 10$ and 20. A similar value has also been found by Haefner & Metz (1982) who combined their lightcurves with radial velocities measured by Wyckhoff & Wehinger (1977). This value for the zero phase is, however, very likely to be influenced by additional emission sources, which give a strong bias at low separations. Wyckhoff & Wehinger state that they derived the radial velocities with “classical methods”, and therefore very probably used the total line for their measurements. Hence, their zero phase can be assumed to be biased in the same way as our values at small d .

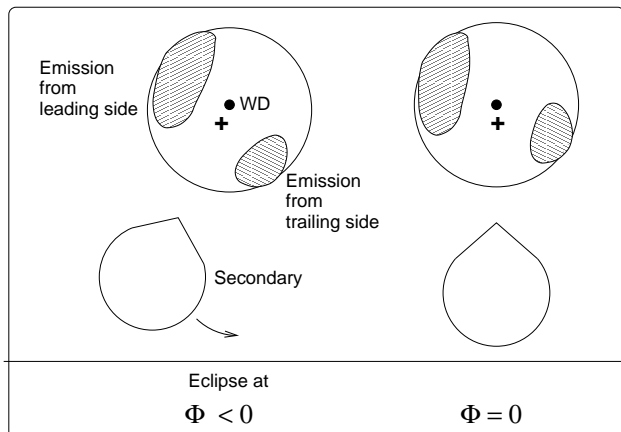


Figure 6. The sketch visualises the geometry of an eclipse (left side) before the superior conjunction of the white dwarf ($\phi_r = 0$, right side). The cross marks the centre of rotation. The eclipsed part has to be an emission source on the leading side of the disc.

For higher separations ($d \sim 30$ and above), which are usually believed to more likely reflect the motion of the white dwarf, the zero phase reaches $\phi_0 = 0.16$ and stays almost constant afterwards. It therefore very likely corresponds to the superior conjunction of the white dwarf and gives an unambiguous input value for the subsequent Doppler mapping. Note that, since the orbital phase was selected in such a way that $\phi_E = 0$ for the eclipse (see Equation 2), the zero phase ϕ_0 indicates the difference between the phase of the eclipse and the zero phase of radial velocities; i.e. the eclipse appears 0.16 orbits before the superior conjunction of the white dwarf (see also Fig. 5). This can only be explained with the assumption that not the disc as a whole is eclipsed, but rather an emission region on the leading side of the disc (Fig. 6).

3.4 Doppler map

For the interpretation of the phase dependent line profiles, the Doppler tomography method as developed by Marsh & Horne (1988) has been applied. A Doppler map $I(v_x, v_y)$ displays the flux emitted by gas moving with the velocity (v_x, v_y) . This deprojection is achieved due to the rotation of the binary system, as the projection of the velocity (v_x, v_y) follows a sinusoidal radial velocity curve. Hence, the line profiles can be transformed into a map $I(v_x, v_y)$ without any assumptions about the actual velocity field.

To correct for the variation of the equivalent width, the input spectra have been normalised by the $\text{H}\alpha$ emission line flux. The intensity values in the Doppler map are hence to be interpreted as relative flux values only. Furthermore, we corrected the orbital phase of the input spectra by the zero value $\phi_0 = 0.16$.

The final Doppler map is given in Fig. 7 and shows the distribution of $\text{H}\alpha$ emission sources in velocity coordinates. Apart from the disc itself, which is clearly visible, two significant additional emission sources can be seen. The orientation of the map is chosen in such a way that the phase angle ϕ_r with respect to the zero point of radial velocities, is zero towards the top and increases clockwise. The smaller of the

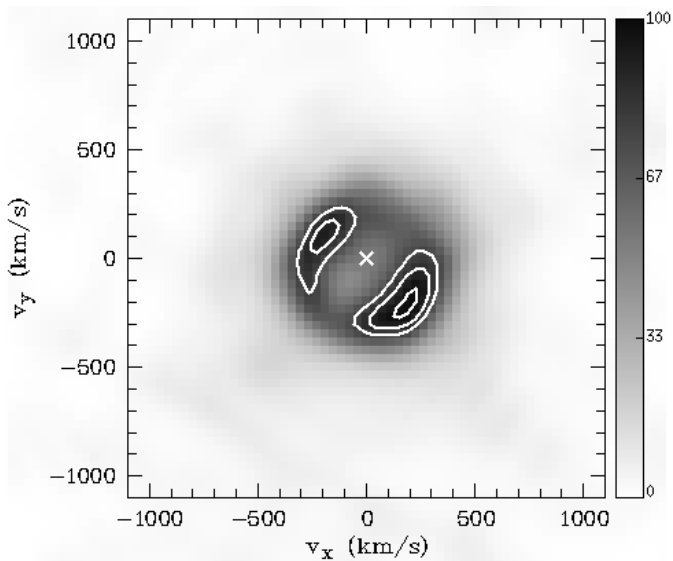


Figure 7. Doppler map of RR Pic showing the distribution of H α -sources in velocity coordinates. The cross marks the centre of rotation, which corresponds to the centre of gravity of the system. The map is oriented in such a way that the phase angle referring to the zero point of radial velocities is zero towards the top and increases clockwise. The contour lines refer to values 75, 85, and 95 and indicate the relative brightness of the emission sources.

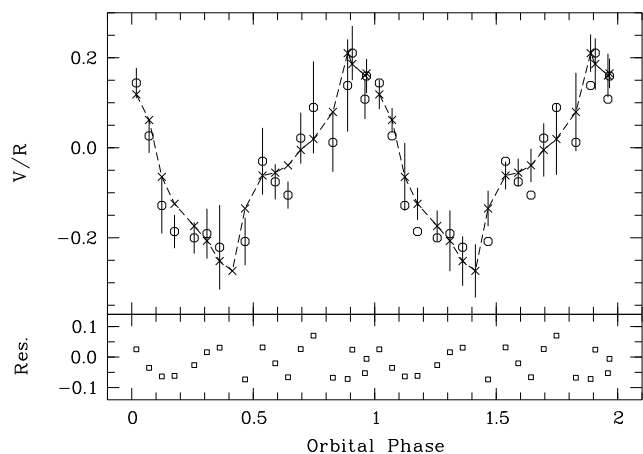


Figure 8. V/R and its residuals is plotted against the orbital phase referring to radial velocity zero point. Error bars have been determined by a Monte Carlo simulation. Two orbits are plotted, the original data (\circ) with error bars between phases 0.0 and 1.0, and the reconstructed (\diamond) one with error bars between phases 1.0 and 2.0. The latter points have additionally been connected via dashed lines.

two emission sources is situated at a phase angle $\phi_r \approx 0.8$, a place that is usually identified with emission from the hot spot. The stronger emission, however, arises on the opposite side, 180° away, at $\phi_r \approx 0.3$.

The quality of the Doppler map can be judged in several ways. In this paper a quantitative approach is made to compare the shape of the emission line in the original and reconstructed spectrum. The asymmetry of the line profile can be measured by a V/R plot. Here, the line profile is divided

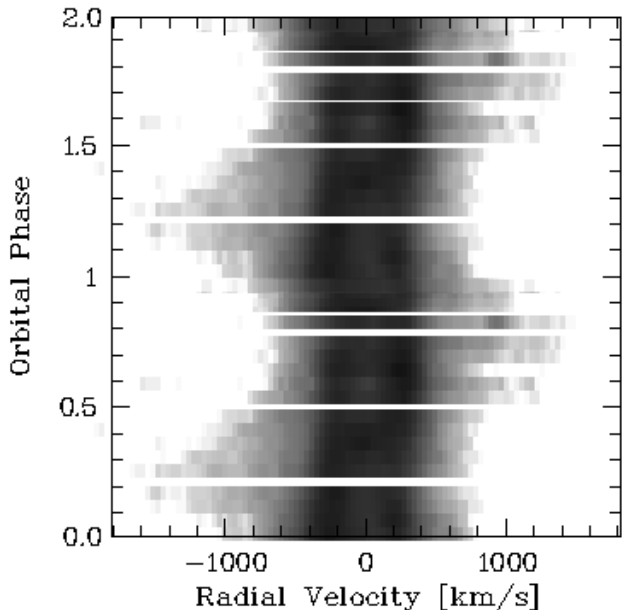


Figure 9. The observed H α emission line profile of RR Pic has been plotted against the phase. The spectra have been flux normalised as described in the text and the wavelength transformed into radial velocities with respect to $\lambda_0 = 6562.8 \text{ \AA}$. Intensities are logarithmically colour coded to favour the display of the faint outer wings. The little enhancement at phase 0.83 and 900 km s^{-1} is due to a not properly subtracted cosmic ray.

in two halves, and V/R defined as logarithm of the ratio of the fluxes in the blue (violet) and red half (Tappert et al. 2002). In Fig. 8, V/R of the original and reconstructed line profile is plotted against the orbital phase. The residuals given below show no sign of periodicity, hence indicating the good quality of the fit.

3.5 High velocity wings

In Fig. 9 the changing line profiles of the flux normalised H α emission line are displayed as an image with emphasis on the faint outer parts of the line. One can clearly see that the line wings reach up to velocities of 1200 km s^{-1} and vary with the orbital phase.

The classical explanation for this feature is that it is caused by gas circling the white dwarf at velocities of about 1200 km s^{-1} . However, there are some problems with this picture. According to Fig. 9, the gas not only has these high velocities, but also changes its velocity by the same magnitude with phase; it is completely on the side of negative velocities at phase $\phi_r = 0.25$ and on the side of positive velocities at $\phi_r = 0.75$. As the high velocity gas is supposed to be in the inner part of the disc, this indicates a semi-amplitude $K_1 \approx 1000 \text{ km s}^{-1}$, which is a very unlikely value, especially as the distance of the white dwarf from the centre of mass in the Doppler map indicates a much smaller K_1 .

Similar high velocity wings have been found in the Balmer lines of the SW Sex-type systems, e.g. LS Peg (Taylor et al. 1999). They explain the wings and their variation with a modified disc-overflow model similar to the one developed by Hellier & Robinson (1994). There are cer-

tainly similarities between RR Pic and SW Sex-type stars, as the orbital period is between 3 h and 4 h and the radial velocity phase lags behind the eclipse phase (which we have explained by an eclipse of the emission source on the leading side). However, the dominant absorption feature around phase 0.5, which is typical for SW Sex-type stars and probably related to the disc-overflow is not present in RR Pic. Also, if all accreted material were deflected over the disc, no hot spot could be present. However, some SW Sex-type stars are known to show emission sources on the trailing side of their discs. Hence the possibility of part of the accretion stream flowing over the disc can not be ruled out for RR Pic.

A different explanation is that the high velocity gas does not stay inside the system but is actually ejected in the form of an asymmetric outflow, with maximum projected velocity of 1200 km s^{-1} . Taking into account the proposed inclination $i = 65^\circ$ (Haefner & Metz 1982) the real outflow velocity has to be around 1350 km s^{-1} . This would explain the variation of the high velocity component as a lighthouse effect: the outflow emerges from one part of the disc only and is swept around with the rotation of the system. In this picture, both the high velocity itself and its varying amplitude are explained in a consistent way. Including the information from phase $\phi_r = 0.25$ of maximal negative velocity (outflow towards us), the origin of the outflow coincides with the position of the isolated emission source on the leading side of the accretion disc. See Fig. 10 for an explanatory sketch.

Additional evidence for the presence of an outflow in RR Pic comes from the mapping of its remnant shell, which shows a bipolar structure in the form of an equatorial ring with some tails orthogonal to it (Gill & O’Brien 1998). Although this map shows the shell far outside the binary, the ring might well be fed by the asymmetric outflow from the binary. The fact that no P Cygni profiles have been found in IUE spectra of RR Pic (Rosino et al. 1982) has been interpreted as RR Pic having no outflow and that the shell is already decoupled from the binary. The asymmetric outflow can be considered as optically thin as it is visible in emission. Any P Cygni absorption has hence to be weak, and can furthermore only be produced during the phase when the outflow is directed towards the observer. It would hence smear out over normal exposure times, and is therefore not in contradiction with the observations.

4 CONCLUSION

We have shown via a Doppler map that two isolated emission sources are present in the disc of RR Pic. Combining the radial velocities with published lightcurves we come to a rather uncommon interpretation of the photometric eclipse as an eclipse of the leading side emission source (see Fig. 6) rather than an eclipse of the hot spot as suggested previously by Kubiak (1984).

Putting all the information together, we confirm the working model of Haefner & Metz (1982) for RR Pic in preference to the one of Vogt (1975). Although, as discussed in section 4, the superior conjunction of the white dwarf takes place 0.1 earlier in phase, this does not change their basic interpretation. Warner’s (1986) doubts of the model were based on the fact that no isolated emission from the leading side had been found in other CVs. Mean-

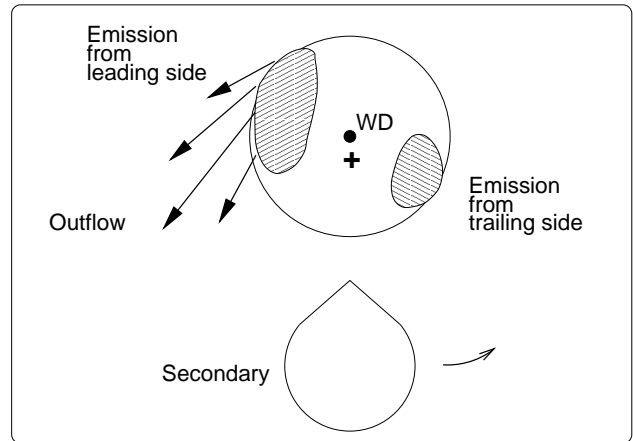


Figure 10. The sketch visualises our model of the emission sources in RR Pic and the outflow coming from the emission region on the leading side of the disc. During a complete orbit of the binary rotation, the projected velocity of the outflow changes between negative (flow towards the observer) and positive (flow away from observer) velocities.

while many systems with this structure have been found (see Tappert & Hanuschik (2001) for an overview), and this argument is no longer valid.

Although common, no convincing explanation for isolated emission sources on the leading side of the disc has so far been presented. Among other possibilities, the presence of spiral shock waves has been discussed as possible explanation for similar features in other CVs (see e.g. Steeghs (2001)). Due to their still enhanced mass transfer, long-period old novae should possess extended hot discs, and are therefore indeed candidates for possessing spiral shocks (Boffin 2001). However, although the emission sources in the disc of RR Pic have a clearly elongated structure, neither time nor spectral resolution of our data is high enough to confirm this picture for RR Pic.

The analysis of the high velocity wings of the $H\alpha$ line yields two possible explanations for these wings and their variability. They may originate from a partial disc-overflow, or from an asymmetric outflow from the accretion disc, i.e. from the emission source on the leading side of the disc. In this case, a connection between the outflow of the binary and the ring-like structure of RR Pic’s shell seems plausible. Deep, high resolution $H\alpha$ images as well as high resolution spectroscopy of some metal lines might help to clarify this picture.

REFERENCES

- Becker R.H., Marshall F.E., 1981, ApJ, 244, L93
- Boffin H.M.J., 2001, in Boffin et al., eds, *Astrotomography*. Lect. Notes on Phys. 573, p. 69
- Gill C.D., O’Brien T.J., 1998, MNRAS, 300, 221
- Haefner R., Metz K., 1982, A&A, 109, 171
- Haefner R., Schoembs R., 1985, A&A, 150, 325
- Haefner R., Betzenbichler W., 1991, IBVS 3665
- Hellier C., Robinson E.L., 1994, ApJ, 431, L107
- Kubiak M., 1984, Acta Astron., 34, 331

- Marsh T.R., Horne K., 1988, MNRAS, 235, 269
Rosini L., Bianchini A., Rafanelli P., 1982, A&A, 108, 243
Scargle J.D., 1982, ApJ, 263, 835
Spencer Jones H., 1931, Cape Obs. Ann., 10, Part 9
Spruit H., 1998, preprint, astro-ph/9806141
Shafter, A.W., 1983, ApJ 267, 222
Steeghs, D., 2001, in Boffin et al., eds, Astrotomography.
Lect. Notes on Phys. 573, 45
Tappert C., 1999, PhD thesis, Ruhruniversität Bochum
Tappert C., Hanuschik R., 2001, in Boffin et al., eds, Astrotomography. Lect. Notes on Phys. 573, 119
Tappert C., Mennickent R., Arenas J., Matsumoto K., Hanuschik R., 2002, submitted to A&A
Taylor C.J., Thorstensen J.R., Patterson J., 1999, PASP, 111, 184
Vogt N., 1975, A&A, 41, 15
Warner B., 1986, MNRAS, 219, 751
Wyckoff S., Wehinger P.A., 1977, in Kippenhahn R. et al., eds, The Interaction of Variable Stars with their Environment, IAU Colloq. 42, p. 201